Double quantum dot as detector of spin bias

Qing-feng Sun,[1] Yanxia Xing,[1] and Shun-Qing Shen[2]
[1]*Beijing National Laboratory for Condensed Matter Physics and Institute of Physics, Chinese Academy of Sciences, Beijing 100190, People's Republic of China*
[2]*Department of Physics, and Center of Theoretical and Computational Physics, the University of Hong Kong, Hong Kong, China*
(Received 10 December 2007; revised manuscript received 6 March 2008; published 13 May 2008)

It was proposed that a double quantum dot can be used as a detector of the spin bias. Electron transport through a double quantum dot is theoretically investigated when a pure spin bias is applied on two conducting leads in contact with the quantum dot. It is found that the spin polarization in the left and right dots may be spontaneously induced, while the intradot levels are located within the spin bias window and breaks the left-right symmetry of the two quantum dots. As a result, a large current emerges. For an open external circuit, a charge bias instead of a charge current will be induced at equilibrium, which is believed to be measurable according to the current nanotechnology. This method may provide a practical and whole electrical approach to detect the spin bias (or the spin current) by measuring the charge bias or current in a double quantum dot.

DOI: 10.1103/PhysRevB.77.195313 PACS number(s): 73.23.−b, 85.75.−d, 73.21.La, 85.35.−p

I. INTRODUCTION

The discovery and application of the giant magnetoresistance in metallic thin films marked the beginning of a new era in spintronics.[1,2] Since then, people have begun to exploit electron spin to replace the role of the electron charge in electronic devices. As a counterpart of the charge current, the spin current, in which spin-up and spin-down electrons coherently move in opposite directions, has attracted extensive interests.[3] Various methods were proposed to generate spin current[4] and to explore the characteristics of the spin transport. Over the last few years, the search for the spin current has made great progress. It has been successfully generated and detected by various means such as optical injection,[5,6] magnetic tunneling injection,[7,8] or spin Hall effect.[9,10] All of these experiments focus on the optical measurement of spin accumulation near the boundaries of the sample or the electric measurement of the scattering effect induced by the spin current via spin-orbital coupling. There are also some proposals to measure spin current or spin-polarized current,[11–14] e.g., to measure the spin torque while a spin current flows through a ferromagnetic-nonmagnetic interface,[11] or to detect the induced electric field by the spin current.[12,13] In all of these methods, the optical, magnetic materials or impurities, magnetic field, or spin-orbit interaction are always involved. Up to now, it is still a challenge to efficiently detect the spin current, which has become a bottleneck for the development of the spintronics.

When a spin current flows through a device, there always exists a spin bias between the two terminals of the device.[15] A spin bias means that the chemical potentials of the two terminals are spin dependent (see Fig. 1). The spin bias is regarded as the driving force behind the spin current. When the circuit is open, the spin current has to be zero. Consequently, the spin bias usually induces the spin accumulation at equilibrium. When the circuit is connected, a spin current circulates. The relation between the spin bias and the spin current is very similar to the relation between the charge bias and the charge current. On the charge transport, people often detect the charge bias to replace the measurement of the charge current. Correspondingly, we can also measure the spin bias instead of just the spin current. In this paper, we propose an effective method to detect the spin bias.

The present proposal is a whole electric measurement of the spin bias by means of a double quantum dot (DQD). It does not involve any optical or magnetic means, or even the spin-orbit interaction. The spin bias can be detected by measuring the (charge) bias. The DQD can be regarded as an artificial molecule and the electron numbers in the DQD can be controlled very well. In the last two decades, the electron transport through the DQD device has been extensively investigated.[16,17] DQD has also been proposed as a qubit,[18] which is a device used to detect various tunneling rates, the spin flip rate,[17,19] and so on. Here, we propose that a DQD can be applied to measure the spin bias or the spin current.

Let us first describe the working mechanism of the DQD as a detector of spin bias. Consider a DQD coupled into two conducting leads. Suppose that a spin bias is applied between the left and right leads. Our task is to *experimentally* measure this spin bias. The spin bias is defined as the spin-dependent chemical potentials of the two leads with $\mu_{L\uparrow}=-\mu_{L\downarrow}=-\mu_{R\uparrow}=\mu_{R\downarrow}=V$ (see Fig. 1).[20] Assume that the left-dot level ϵ_L is set at zero and the right-dot level ϵ_R is at $-U$, where U is the intradot electron-electron (e-e) Coulomb interaction. This particular level position is chosen to demonstrate the physics in our proposal and is not necessary at all in a general case. The left dot has a spin-up electron because $\mu_{L\uparrow}>\epsilon_L>\mu_{L\downarrow}$, while the right dot, because $\mu_{R\downarrow}>\epsilon_R+U>\mu_{R\uparrow}>\epsilon_R$, is occupied by a spin-down electron, and its spin-up level is consequently pushed away to the higher energy ϵ_R+U and is

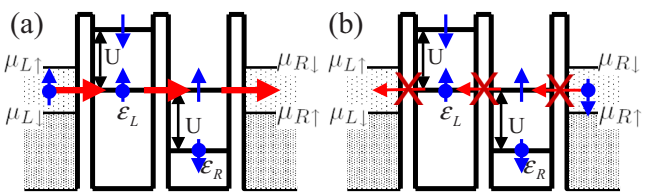

FIG. 1. (Color online) [(a) and (b)] The schematic plots illustrate a spin-up (spin-down) electron tunneling from the left (right) to the right (left) lead.

empty (see Fig. 1). The spin-up electron can then tunnel from the left lead via the two dots to the right lead [see Fig. 1(a)]. Oppositely, the spin-down electron can hardly flow from the right lead to the left lead because of the Pauli exclusion principle and the occupancy of the spin-down level in the right dot [see Fig. 1(b)]. This breaks the symmetry of the motion of spin-up and spin-down electrons in a pure spin bias. As a result, a (charge) current circulates. This induced current can be experimentally measured and consequently be applied to measure the spin bias.

The paper is organized as follows: In Sec. II, the model for the DQD and the general formalism for the nonequilibrium Keldysh Green's function method are presented. The spin-bias-induced charge current J and the electron occupation numbers in the DQD are calculated. In Sec. III, we take the numerical investigation. The spin-dependent charge stability diagram, in terms of the spin bias, is obtained. In Sec. IV, the induced charge bias in an open circuit is numerically studied. Finally, a brief summary is presented in Sec. V.

II. MODEL AND FORMULATION

In this section, we present the model Hamiltonian of this DQD and the general formalism of Keldysh Green's function technique for electron transport through the DQD. The DQD device is modeled by the following Hamiltonian:

$$H = \sum_{\alpha,k,\sigma} \epsilon_{\alpha k} a^{\dagger}_{\alpha k\sigma} a_{\alpha k\sigma} + \sum_{\alpha,\sigma} \epsilon_{\alpha} d^{\dagger}_{\alpha\sigma} d_{\alpha\sigma} + \sum_{\alpha} U_{\mathrm{in}} d^{\dagger}_{\alpha\uparrow} d_{\alpha\uparrow} d^{\dagger}_{\alpha\downarrow} d_{\alpha\downarrow} + \sum_{\sigma,\sigma'} U_{ex} d^{\dagger}_{L\sigma} d_{L\sigma} d^{\dagger}_{R\sigma'} d_{R\sigma'} + \sum_{\alpha,k,\sigma} t_{\alpha} a^{\dagger}_{\alpha k\sigma} d_{\alpha\sigma} + \sum_{\sigma} t_c d^{\dagger}_{L\sigma} d_{R\sigma} + \mathrm{H.c.}, \quad (1)$$

where $a^{\dagger}_{\alpha k\sigma}$ ($a_{\alpha k\sigma}$) and $d^{\dagger}_{\alpha\sigma}$ ($d_{\alpha\sigma}$) are the creation (annihilation) operators of an electron with spin $\sigma(=\uparrow,\downarrow)$ in the lead $\alpha(=L,R)$ and the dot α, respectively. Each dot has a single energy level ϵ_{α} and an intradot e-e interaction U_{in}. In addition, the interdot e-e interaction U_{ex} is also included. We emphasize that the system does not break the spin SU(2) symmetry and the hopping coefficients t_{α} and t_c are spin independent.

Following the transport theory of Keldysh Green's function,[21] the electron current $J_{\alpha\sigma}$ with the spin σ from the lead α flowing into the dot α and the occupation number of electrons, $n_{\alpha\sigma}$, at the level α,σ can be expressed as

$$J_{\alpha\sigma} = -\,\mathrm{Im} \int \frac{d\epsilon}{2\pi} \Gamma_{\alpha} [2 f_{\alpha\sigma} G^{r}_{\alpha\alpha\sigma}(\epsilon) + G^{<}_{\alpha\alpha\sigma}(\epsilon)], \quad (2)$$

$$n_{\alpha\sigma} = \langle d^{\dagger}_{\alpha\sigma} d_{\alpha\sigma} \rangle = -\,i \int \frac{d\epsilon}{2\pi} G^{<}_{\alpha\alpha\sigma}(\epsilon), \quad (3)$$

where $\Gamma_{\alpha} = 2\pi \Sigma_k |t_{\alpha}|^2 \delta(\epsilon - \epsilon_{\alpha k})$. $f_{\alpha\sigma}(\epsilon) = 1/\{\exp[(\epsilon - \mu_{\alpha\sigma})/k_B T] + 1\}$ is the Fermi–Dirac distribution of electrons in the leads. Because of the spin bias in the two leads, the chemical potentials for spin-up and spin-down electrons are not equal. $G^{r}_{\alpha\alpha\sigma}(\epsilon)$ and $G^{<}_{\alpha\alpha\sigma}(\epsilon)$ in Eqs. (2) and (3) are the standard retarded and Keldysh Green's functions of the QDs; they are the Fourier transformation of $G^{r,<}_{\alpha\alpha\sigma}(t)$, where

$$G^{r}_{\alpha\alpha'\sigma}(t) \equiv -\,i\theta(t) \langle \{ d_{\alpha\sigma}(t), d^{\dagger}_{\alpha'\sigma}(0) \} \rangle,$$

$$G^{<}_{\alpha\alpha'\sigma}(t) \equiv i \langle d^{\dagger}_{\alpha\sigma}(0) d_{\alpha'\sigma}(t) \rangle.$$

We first solve Green's functions $\mathbf{g}^{r}_{\sigma}(\epsilon)$ of the isolated DQD system (i.e., $t_{\alpha} = t_c = 0$). Consider that the spin bias V is less than the intradot e-e interaction U_{in} and the two-electron cotunneling events can be ignored. $\mathbf{g}^{r}_{\sigma}(\epsilon)$ are obtained from the equation of motion technique,[22]

$$g^{r}_{\alpha\alpha\sigma}(\epsilon) = \frac{(1 - n_{\alpha\bar{\sigma}})(1 - \{n_{\bar{\alpha}}\})}{A} + \frac{(1 - n_{\alpha\bar{\sigma}})\{n_{\bar{\alpha}}\}}{A - U_{\mathrm{ex}}} + \frac{n_{\alpha\bar{\sigma}}(1 - \{n_{\bar{\alpha}}\})}{A - U_{\mathrm{in}}} + \frac{n_{\alpha\bar{\sigma}}\{n_{\bar{\alpha}}\}}{A - U_{\mathrm{in}} - U_{\mathrm{ex}}}, \quad (4)$$

and $g^{r}_{LR\sigma} = g^{r}_{RL\sigma} = 0$, where $\bar{\alpha} = R$ for $\alpha = L$ and $\bar{\alpha} = L$ for $\alpha = R$, $\bar{\sigma} = \downarrow$ for $\sigma = \uparrow$ and $\bar{\sigma} = \uparrow$ for $\sigma = \downarrow$, $A \equiv \epsilon - \epsilon_{\alpha} - [n_{\bar{\alpha}}] U_{\mathrm{ex}} + i0^{+}$, $\{n_{\bar{\alpha}}\} \equiv n_{\bar{\alpha}} - [n_{\bar{\alpha}}]$, and $[n_{\alpha}]$ is the integer part of n_{α}. $n_{\alpha} = n_{\alpha\uparrow} + n_{\alpha\downarrow}$ is the total occupation number of electrons in the dot α. After solving $\mathbf{g}^{r}_{\sigma}(\epsilon)$ of the isolated DQDs, $G^{r}_{\alpha\alpha\sigma}(\epsilon)$ and $G^{<}_{\alpha\alpha\sigma}(\epsilon)$ for the whole system can be obtained from the Dyson and Keldysh equations,[23]

$$\mathbf{G}^{r}_{\sigma}(\epsilon) \equiv \begin{pmatrix} G^{r}_{LL\sigma} & G^{r}_{LR\sigma} \\ G^{r}_{RL\sigma} & G^{r}_{RR\sigma} \end{pmatrix} = \mathbf{g}^{r}_{\sigma}(\epsilon) + \mathbf{g}^{r}_{\sigma}(\epsilon) \boldsymbol{\Sigma}^{r}_{\sigma} \mathbf{G}^{r}_{\sigma}(\epsilon), \quad (5)$$

$$\mathbf{G}^{<}_{\sigma}(\epsilon) \equiv \begin{pmatrix} G^{<}_{LL\sigma} & G^{<}_{LR\sigma} \\ G^{<}_{RL\sigma} & G^{<}_{RR\sigma} \end{pmatrix} = \mathbf{G}^{r}_{\sigma}(\epsilon) \boldsymbol{\Sigma}^{<}_{\sigma}(\epsilon) \mathbf{G}^{a}_{\sigma}(\epsilon). \quad (6)$$

Here, the boldface letters ($\mathbf{G}$, g, and $\boldsymbol{\Sigma}$) represent the 2×2 matrix and the self-energies $\boldsymbol{\Sigma}^{r,<}_{\sigma}(\epsilon)$ are

$$\boldsymbol{\Sigma}^{r}_{\sigma}(\epsilon) = \begin{pmatrix} -i\Gamma_L/2 & t_c \\ t_c & -i\Gamma_R/2 \end{pmatrix}, \quad (7)$$

$$\boldsymbol{\Sigma}^{<}_{\sigma}(\epsilon) = \begin{pmatrix} i\Gamma_L f_{L\sigma}(\epsilon) & 0 \\ 0 & i\Gamma_R f_{R\sigma}(\epsilon) \end{pmatrix}. \quad (8)$$

Equations (3)–(6) can be self-consistently solved. The (charge) current through the DQD is given by

$$J = e(J_{L\uparrow} + J_{L\downarrow}) = -\,e(J_{R\uparrow} + J_{R\downarrow}).$$

Finally, it is worth pointing out that the present problem can be solved by other means, such as, for example, the rate equation method.[24]

III. SPIN-DEPENDENT CHARGE STABILITY DIAGRAM AND CHARGE CURRENT

Before presenting numerical results, we emphasize that the spin bias we apply to the DQD device is a pure symmetric one without a (charge) bias, i.e., $\mu_{L\uparrow} + \mu_{L\downarrow} = \mu_{R\uparrow} + \mu_{R\downarrow} = 0$.[20] So if the spontaneously spin-polarized occupations are not induced in the DQD, the charge current J must be zero because of the symmetric behaviors for the motion of the spin-up and the spin-down

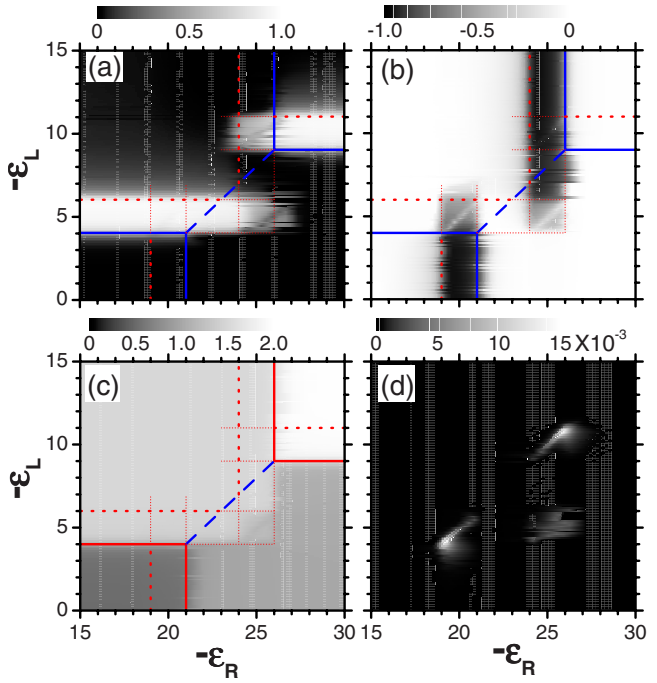

FIG. 2. (Color online) (a) The spin polarization Δn_L at the left dot, (b) Δn_R at the right dot, (c) $n_L+n_R/2$, and (d) the current J as a function of the energy levels ϵ_L and ϵ_R in the two quantum dots. The parameters are $\Gamma_L=\Gamma_R=0.3$, $t_c=T=0.1$, $U_{\text{in}}=20$, $U_{\text{ex}}=5$, and $V=1$.

electrons. For example, in the case of a single quantum dot instead of the DQDs applied by the pure spin bias, there is no spin polarization in the dot and the current is always zero as the spin up-down symmetry is retained. So, in the following, we first investigate the stability diagram of the spin polarization and the spin-dependent charge density in the DQD.

Figures 2(a) and 2(b) present the spin polarizations Δn_α ($\Delta n_\alpha \equiv n_{\alpha\uparrow}-n_{\alpha\downarrow}$) of the left and right dots versus the levels ϵ_L and ϵ_R, and Fig. 2(c) presents the occupation number of electrons, $n_L+n_R/2$.[25] It is found that these quantities are determined by the relative energy levels of ϵ_L and ϵ_R. The spin polarization Δn_α is indeed nonzero and is even quite large (i.e., near ± 1) in some specific regions. Let us analyze the spin-dependent charge stability diagram [see Fig. 3(a)], which gives the spin-dependent occupation numbers of electrons as a function of ϵ_L and ϵ_R. If it is without a spin bias ($V=0$), there are four domains (0,1), (1,1), (0,2), and (1,2) in the stability diagram [see the thin dashed curves in Fig. 3(a)], with (n,m) representing n and m electrons in the left and right dots. This type of charge stability diagram has been experimentally observed[16,17] and is well established. While the spin bias V is turned on and the level ϵ_L or ϵ_R is located between $-V$ and $+V$, in addition to the four old spin-unpolarized domains (n,m) with a shift V of their boundaries shift, there appears to be four spin-polarized domains, which are denoted by $(\uparrow,1)$, $(0,\downarrow)$, $(1,\downarrow)$, and $(\uparrow,2)$. The notation $(\uparrow,1)$, for example, represents a spin-up electron in the left dot and a spin-unpolarized electron in the right dot.

This spin-dependent charge stability diagram in Fig. 3(a) can be obtained by calculating the electrochemical potentials of the DQD or by analyzing the position level relative to the

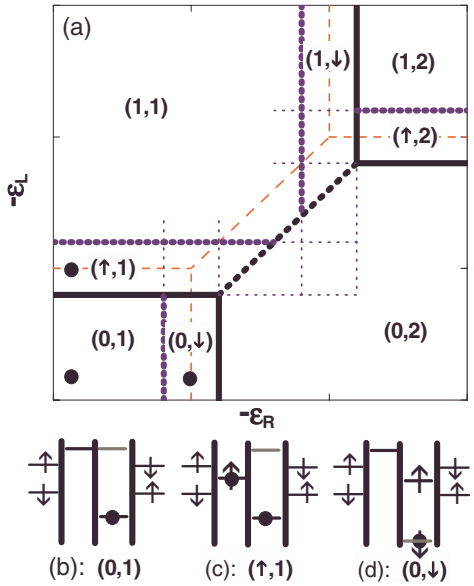

FIG. 3. (Color online) (a) Schematic stability diagram of the DQD under the finite spin bias V. The thin dashed lines are the stability diagram, while $V=0$. [(b)–(d)] are location schematics of energy levels in the (0,1), $(\uparrow,1)$, and $(0,\downarrow)$ domains, respectively.

spin-dependent chemical potentials $\mu_{\alpha\sigma}$. Consider an isolated DQD device with $\Gamma_L=\Gamma_R=t_c=0$. (i) The domain (0,1): when the equivalent level $\tilde{\epsilon}_L$ ($\tilde{\epsilon}_L \equiv \epsilon_L+U_{\text{ex}}$) of the left dot is higher than $\mu_{L\uparrow}$ and $\mu_{L\downarrow}$ and the level ϵ_R of the right dot satisfies $\epsilon_R<\epsilon_L,\mu_{R\uparrow},\mu_{R\downarrow}<\epsilon_R+U_{\text{in}}$ [see Fig. 3(b)], the right dot is occupied by a spin-unpolarized electron and the left dot is empty. (ii) The domain $(\uparrow,1)$: while $\mu_{L\downarrow}<\tilde{\epsilon}_L<\mu_{L\uparrow}$ and $\epsilon_R<\mu_{R\uparrow},\mu_{R\downarrow}<\epsilon_R+U_{\text{in}}$ [see Fig. 3(c)], a spin-up electron occupies the left dot and a spin-unpolarized electron is in the right dot. (iii) The domain $(0,\downarrow)$: if $\tilde{\epsilon}_L>\mu_{L\uparrow},\mu_{L\downarrow}$ and $\mu_{R\uparrow}<\epsilon_R+U_{\text{in}}<\mu_{R\downarrow}$ [see Fig. 3(d)], the left dot is empty. For the right dot, a spin-down electron occupies the level ϵ_R because $\epsilon_R,\epsilon_R+U_{\text{in}}<\mu_{R\downarrow}$, then the spin-up level of the right dot is pushed to ϵ_R+U_{in}, which is over $\mu_{R\uparrow}$, and so it is empty. Similarly, the other five domains can also be obtained. In the case of the finite coupling case $\Gamma_L,\Gamma_R,t_c\neq 0$, the spin-polarized domains slightly extend to the spin-unpolarized domains, as illustrated by the thin dotted lines in Fig. 3(a). Numerical results for the spin polarizations Δn_α [Figs. 2(a) and 2(b)] and the occupation numbers of electrons $n_L+n_R/2$ [Fig. 2(c)] are in good agreement with the charge stability diagram in [Fig. 3(a)]. The eight domains, including four spin-unpolarized and four spin-polarized domains, are clearly visible.

In an alternative way, the stability diagram of Fig. 3(a) can also be deduced from the total energy of the DQD system and the electrochemical potentials. When the isolated DQD is in the states of $\vec{N}=(N_{L\uparrow},N_{L\downarrow},N_{R\uparrow},N_{R\downarrow})$, where $N_{\alpha\sigma}=0$ or 1 is the index of the electron occupation number in the intradot level $\alpha\sigma$, its total energy E_T is

$$E_T(\vec{N}) = N_L\epsilon_L + N_R\epsilon_R + N_L N_R U_{\text{ex}} + (N_{L\uparrow}N_{L\downarrow} + N_{R\uparrow}N_{R\downarrow})U_{\text{in}}, \tag{9}$$

where $N_\alpha=N_{\alpha\uparrow}+N_{\alpha\downarrow}$. Consider the fact that the occupation number in the intradot level $\alpha\sigma$ is mainly affected by the

lead (i.e., electron reservoir) $\alpha\sigma$. The grand thermodynamic potential Ω at zero temperature is

$$\Omega(\vec{N}) = E_T(\vec{N}) - N_{L\uparrow}\mu_{L\uparrow} - N_{L\downarrow}\mu_{L\downarrow} - N_{R\uparrow}\mu_{R\uparrow} - N_{R\downarrow}\mu_{R\downarrow}. \tag{10}$$

In the present system, the electron occupation number can change with the levels ϵ_L and ϵ_R. This is a grand canonical ensemble. Then the stablest state is the one whose grand thermodynamic potential Ω has minimal values and can be straightforwardly found. For the sake of convenience and intuition, we introduce the electrochemical potentials $\mu_{QD\alpha\sigma}$, following Ref. 16. $\mu_{QD\alpha\sigma}$ of the level $\alpha\sigma$ is well defined, for example,

$$\mu_{QDL\uparrow}(\vec{N}) = E_T(\vec{N}) - E_T(N_{L\uparrow} - 1, N_{L\downarrow}, N_{R\uparrow}, N_{R\downarrow}). \tag{11}$$

Then the stablest states are the maximal values of $\vec{N}$, for which four $\mu_{QD\alpha\sigma}(\vec{N})$ are less than the corresponding chemical potentials $\mu_{\alpha\sigma}$. If two states of $\vec{N}$, e.g., $\vec{N}=(0,0,1,0)$ and (0, 0, 0, 1), satisfy the above four equations, they are assumed to have the same probability to exist. A detailed analysis of $\mu_{QD\alpha\sigma}$ versus the parameters ϵ_L and ϵ_R leads to establish the same charge stability diagram, as shown in Fig. 3(a). In fact, the electrochemical potentials $\mu_{QD\alpha\sigma}$ are equal to the equivalent levels in the preceding paragraph. For example,

$$\mu_{QDL\uparrow}(1,0,1,0) = \mu_{QDL\uparrow}(1,0,0,1) = \mu_{QDL\downarrow}(0,1,1,0) = \mu_{QDL\downarrow}(0,1,0,1) = \epsilon_L + U_{ex} = \tilde{\epsilon}_L.$$

In particular, there are only four equivalent levels, which are less than the numbers of $\mu_{QD\alpha\sigma}$. So it is convenient and intuitive to use the equivalent levels to deduce the stability diagram.

With the spin-polarized stability diagram in mind, we turn to calculate the (charge) current J induced by the spin bias. Figure 2(d) shows the current J as a function of the levels ϵ_L and ϵ_R. The current becomes quite large when both the left and right dots are spin polarized, as in the case of $-V<\tilde{\epsilon}_L=\epsilon_R+U_{\text{in}}<V$. The physical origin of the generation of the current has been explained in detail in Sec. I, as shown in Fig. 1. We can establish a relation between the charge current and the spin bias in the two leads. In this way, we can detect the spin bias V by measuring the current J. In the following, we calculate the current for various parameters. Figure 4(a) shows the current J versus the spin bias V for the interdot interaction $U_{\text{ex}}=5$. While $V=0$, J is exactly zero. With the increase in V from zero, the current J first increases, reaches at a maximum, and then drops. J keeps a relatively large value even if V is comparable to the e-e interaction energy U_{in}. The origin of the drop is that the spin polarizations in the two dots decay while the current flows through the DQDs at the large V. In the absence of the interdot e-e interaction U_{ex}, i.e., $U_{\text{ex}}=0$, the current monotonously increases with the spin bias V [see Fig. 4(b)]. In this case, the current J and the spin bias V have one-to-one correspondence. Therefore, the spin bias V can be straightforwardly deduced from the measured current. Figure 4(c) shows the current J as a function of the level ϵ_R of the right dot. When ϵ_R+U_{in} departs $\tilde{\epsilon}_L$ over a few

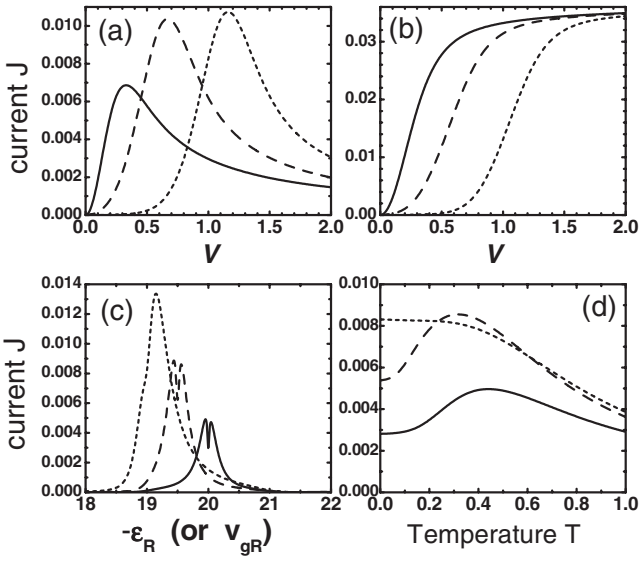

FIG. 4. The current J vs the spin bias V for two interdot interactions (a) $U_{\text{ex}}=5$ and (b) $U_{\text{ex}}=0$. (c) The current J vs the level ϵ_R and (d) the current J vs the temperature T. The solid, dashed, and dotted curves are for levels at $\tilde{\epsilon}_L=0$ and $\epsilon_R=-20$, $\tilde{\epsilon}_L=0.5$ and $\epsilon_R=-19.5$, and $\tilde{\epsilon}_L=1$ and $\epsilon_R=-19$, respectively. The other parameters are the same as in Fig. 2.

Γ_α (e.g., $|\epsilon_R+U_{\text{in}}-\tilde{\epsilon}_L|>3\Gamma_\alpha$), J becomes very small because the tunneling process in Fig. 1(a) is quickly suppressed when ϵ_R+U_{in} is not in alignment with $\tilde{\epsilon}_L$. On the other hand, the tunneling process in Fig. 1(a) frequently occurs and J becomes large when ϵ_R+U_{in} is located near $\tilde{\epsilon}_L$. However, when $\epsilon_R+U_{\text{in}}=\tilde{\epsilon}_L$, J may slightly drop and a dip emerges in the curve of $J-\epsilon_R$ because the spin polarization Δn_α is suppressed at the point. Figure 4(d) displays the current J as a function of temperature T. Here, J slightly depends on the temperature T and is quite large when $T<V$.

IV. CHARGE BIAS IN AN OPEN CIRCUIT

In Sec. III, we calculated the charge current through a DQD induced by a pure spin bias. In an open circuit, the situation will change. At the time that a spin bias is turned on, a charge current will circulate. For an open circuit, the extra charge will accumulate in the two leads until the system reaches a balance. As a result, an extra charge bias V_e, instead of a charge current, will be generated while the charge current vanishes. In this case, the combination of the spin bias V and the induced charge bias V_e will give the spin-dependent chemical potentials $\mu_{\alpha\sigma}$ in the two leads,

$$\mu_{L\uparrow} = +V + V_e, \tag{12a}$$

$$\mu_{L\downarrow} = -V + V_e, \tag{12b}$$

$$\mu_{R\uparrow} = -V - V_e, \tag{12c}$$

$$\mu_{R\downarrow} = +V - V_e. \tag{12d}$$

The bias V_e can be determined by the condition of

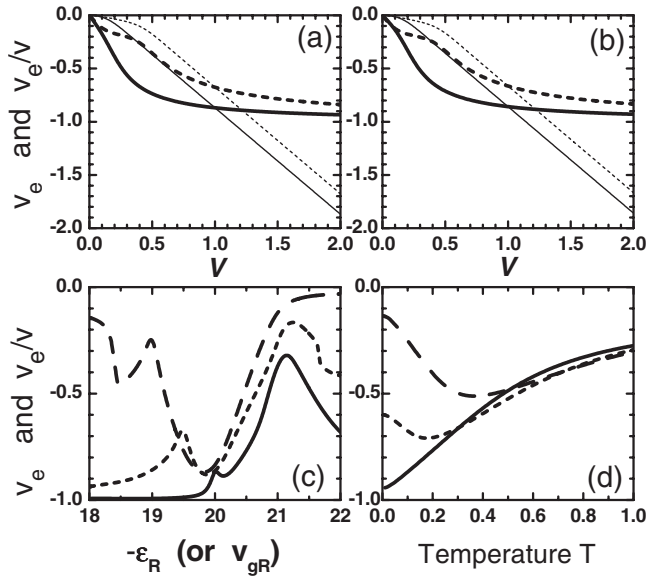

FIG. 5. The induced charge bias V_e (thin curves) and V_e/V (thick curves) vs the spin bias V for interdot interaction (a) $U_{\mathrm{ex}}=5$ and (b) $U_{\mathrm{ex}}=0$. (c) V_e (i.e., V_e/V) vs the level ϵ_R and (d) V_e (i.e., V_e/V) vs the temperature T. The solid, dashed, and dotted curves are for levels at $\tilde{\epsilon}_L=0$ and $\epsilon_R=-20$, $\tilde{\epsilon}_L=0.5$ and $\epsilon_R=-19.5$, and $\tilde{\epsilon}_L=1$ and $\epsilon_R=-19$, respectively. The other parameters are the same as in Fig. 2

$$J=0 \tag{13}$$

at equilibrium for the open circuit. Figures 5(a) and 5(b) gives the bias V_e and V_e/V versus the spin bias V in the presence and absence of the intradot Coulomb interaction U_{ex}. $|V_e|$ and $|V_e/V|$ monotonously increase with V regardless of the value of U_{ex}. This is different from the curve of J-V, in which J drops down for a large V while $U_{\mathrm{ex}}\neq 0$ [see Fig. 4(a)]. This illustrates that it is more efficient to measure the induced bias V_e than to measure the induced current J. Figure 5(c) shows the bias V_e as a function of the level ϵ_R. The bias $|V_e|$ always has a large value (e.g., $|V_e/V|>0.1$), even if $\epsilon_R+U_{\mathrm{in}}$ is far away from $\tilde{\epsilon}_L$. Notice that the current J is relatively small when $|\epsilon_R+U_{\mathrm{in}}-\tilde{\epsilon}_L|>3\Gamma_\alpha$ [see Fig. 4(c)]. The transmission coefficient (or the conductance) is also very small in this region. Correspondingly, V_e in an open circuit is still large. Therefore, the induced bias V_e can be measured in a more extensive region. Figure 5(d) gives the temperature T dependence of the bias V_e, which is almost independent of the temperature T. Finally, we emphasize that $|V_e/V|$ is usually larger than 0.1 regardless of the values of the parameters V, ϵ_L, ϵ_R, T, etc. In the current technology, the bias in the order of 0.1 nV is measurable in the experiment.[26] Therefore, if the spin bias V, i.e., the difference between the spin-up and spin-down chemical potentials $(\mu_{L\uparrow}-\mu_{L\downarrow})/e$, reaches 1 nV, the induced bias in the present calculation is large enough to be measured in the experiment.

V. CONCLUSIONS

In summary, we investigated the electron transport driven by a spin bias or pure spin current through a nonmagnetic DQD. Except for spin-unpolarized domains, several spin-polarized domains are found in the stability diagram with respect to the energy levels of two quantum dots. When both the left and right dots are spin polarized, a large charge current J can be induced by applying a pure spin bias. In particular, in an open circuit, the charge bias is induced to balance the spin bias and is measurable in an extensive range of the parameters. Physically, a pure spin bias may drive electrons with a different spin in the opposite direction. If the system possesses the left-right symmetry or parity and does not break the time reversal symmetry, it will circulate a pure spin current (or spin accumulation in an open circuit). When the energy levels in the two dots are not equal, the left-right symmetry or parity of the system is broken. A spin bias and a strong Coulomb interaction can produce two spin-polarized states in the two dots, as we discussed in the spin-polarized charge stability diagram. As a result, the currents with different spins in opposite directions will not be equal anymore. Consequently, this pure spin bias generates a charge current through the DQD. This property may provide a practical approach to detect the spin bias in the DQD by measuring the charge bias or charge current.

ACKNOWLEDGMENTS

We acknowledge the financial support from NSF-China under Grants No. 10525418, No. 10734110, and No. 60776060 (Q.F.S.), and the Research Grant Council of Hong Kong under Grant No. HKU 7041/07P (S.Q.S.). Q.F.S. would like to thank W. Long for many helpful discussions.

[1] S. A. Wolf, D. D. Awschalom, R. A. Buhrman, J. M. Daughton, S. von Molnár, M. L. Roukes, A. Y. Chtchelkanova, and D. M. Treger, Science **294**, 1488 (2001); Gary A. Prinz, *ibid.* **282**, 1660 (1998).

[2] I. Zutic, J. Fabian, and S. Das Sarma, Rev. Mod. Phys. **76**, 323 (2004).

[3] D. D. Awschalom and M. E. Flatte, Nat. Phys. **3**, 153 (2007).

[4] R. D. R. Bhat and J. E. Sipe, Phys. Rev. Lett. **85**, 5432 (2000); Q.-F. Sun, H. Guo, and J. Wang, *ibid.* **90**, 258301 (2003); P. Sharma and P. W. Brouwer, *ibid.* **91**, 166801 (2003); Susan K. Watson, R. M. Potok, C. M. Marcus, and V. Umansky, *ibid.* **91**, 258301 (2003); W. Long and Q.-F. Sun, Hong Guo, and J. Wang, Appl. Phys. Lett. **83**, 1397 (2003).

[5] J. Hübner, W. W. Rühle, M. Klude, D. Hommel, R. D. R. Bhat, J. E. Sipe, and H. M. van Driel, Phys. Rev. Lett. **90**, 216601 (2003); M. J. Stevens, Arthur L. Smirl, R. D. R. Bhat, Ali Najmaie, J. E. Sipe, and H. M. van Driel, *ibid.* **90**, 136603 (2003).

[6] X. D. Cui, S.-Q. Shen, J. Li, Y. Ji, W. K. Ge, and F.-C. Zhang, Appl. Phys. Lett. **90**, 242115 (2007); J. Li, X. Dai, S.-Q. Shen, and F.-C. Zhang, *ibid.* **88**, 162105 (2006).

[7] S. O. Valenzuela and M. Tinkham, Nature (London) **442**, 176 (2006).
[8] T. Kimura, Y. Otani, T. Sato, S. Takahashi, and S. Maekawa, Phys. Rev. Lett. **98**, 156601 (2007); E. Saitoh, M. Ueda, H. Miyajima, and G. Tatara, Appl. Phys. Lett. **88**, 182509 (2006).
[9] Y. K. Kato, R. C. Myers, A. C. Gossard, and D. D. Awschalom, Science **306**, 1910 (2004); V. Sih, R. C. Myers, Y. K. Kato, W. H. Lau, A. C. Gossard, and D. D. Awschalom, Nat. Phys. **1**, 31 (2005); V. Sih, W. H. Lau, R. C. Myers, V. R. Horowitz, A. C. Gossard, and D. D. Awschalom, Phys. Rev. Lett. **97**, 096605 (2006).
[10] J. Wunderlich, B. Kaestner, J. Sinova, and T. Jungwirth, Phys. Rev. Lett. **94**, 047204 (2005).
[11] P. Mohanty, G. Zolfagharkhani, S. Kettemann, and P. Fulde, Phys. Rev. B **70**, 195301 (2004); Tsung-Wei Chen, Chih-Meng Huang, and G. Y. Guo, *ibid.* **73**, 235309 (2006).
[12] F. Meier and D. Loss, Phys. Rev. Lett. **90**, 167204 (2003); F. Schütz, M. Kollar, and P. Kopietz, *ibid.* **91**, 017205 (2003).
[13] Q.-F. Sun, H. Guo, and J. Wang, Phys. Rev. B **69**, 054409 (2004); Q.-F. Sun and X. C. Xie, *ibid.* **72**, 245305 (2005).
[14] G. Bergmann, Phys. Rev. B **63**, 193101 (2001); A. G. Mal'shukov, C. S. Tang, C. S. Chu, and K. A. Chao, *ibid.* **68**, 233307 (2003); S. I. Erlingsson and D. Loss, *ibid.* **72**, 121310(R) (2005).
[15] For the persistent spin current in an equilibrium system, the spin bias is always zero, which is very similar to the supercurrent in a superconducting state. So the method in the present paper cannot be applied to detect the persistent spin current. The potential measurement methods for this type of spin current are referred to Q.-F. Sun, X. C. Xie, and J. Wang, Phys. Rev. Lett. **98**, 196801 (2007); Phys. Rev. B **77**, 035327 (2008), and references therein.
[16] W. G. van der Wiel, S. De Franceschi, J. M. Elzerman, T. Fujisawa, S. Tarucha, and L. P. Kouwenhoven, Rev. Mod. Phys. **75**, 1 (2002).
[17] R. Hanson, L. P. Kouwenhoven, J. R. Petta, S. Tarucha, and L. M. K. Vandersypen, Rev. Mod. Phys. **79**, 1217 (2007).
[18] D. Loss and D. P. DiVincenzo, Phys. Rev. A **57**, 120 (1998); A. Imamoglu, D. D. Awschalom, G. Burkard, D. P. DiVincenzo, D. Loss, M. Sherwin, and A. Small, Phys. Rev. Lett. **83**, 4204 (1999); B. Burkard and D. Loss, in *Semiconductor Spintronics and Quantum Computation*, edited by D. D. Awschalom, D. Loss, and N. Samarth (Springer-Verlag, Berlin, 2002), Chap. 8.
[19] K. Ono and S. Tarucha, Phys. Rev. Lett. **92**, 256803 (2004).
[20] D.-K. Wang, Q.-F. Sun, and H. Guo, Phys. Rev. B **69**, 205312 (2004).
[21] Y. Meir and N. S. Wingreen, Phys. Rev. Lett. **68**, 2512 (1992).
[22] Here, we took the approximation $\langle \hat{n}_{L\sigma}\hat{n}_{R\sigma'}\rangle = \langle \hat{n}_{L\sigma}\rangle\langle \hat{n}_{R\sigma'}\rangle = n_{L\sigma}n_{R\sigma'}$ and $\langle \hat{n}_{\alpha\uparrow}\hat{n}_{\alpha\downarrow}\rangle = 0$ while $0 < n_\alpha < 1$ and $\langle \hat{n}_{\alpha\uparrow}\hat{n}_{\alpha\downarrow}\rangle = n_\alpha - 1$ while $1 < n_\alpha < 2$, where $\hat{n}_{\alpha\sigma} \equiv d^\dagger_{\alpha\sigma}d_{\alpha\sigma}$. Because of $V < U_{\text{in}}$, the fluctuation in the occupation number is less than one in each dot and the approximation should be reasonable.
[23] This system with e-e interactions in the nonequilibrium case (e.g., with the non-zero spin bias) is not exactly solvable. One has to introduce some approximations. In Eqs. (5) and (6), we have neglected the higher order of self-energy correction that originates from the combination of the e-e interaction and the hopping terms. This approximation is much better than the Hartree–Fork approximation. When the hopping coefficients (t_α and t_c) are weak or when the system is not in the Kondo regime, this method is expected to work very well, e.g., see A. Groshev, T. Ivanov, and V. Valtchinov, Phys. Rev. Lett. **66**, 1082 (1991); Q.-F. Sun and X. C. Xie, Phys. Rev. B **73**, 235301 (2006).
[24] S. A. Gurvitz and Ya. S. Prager, Phys. Rev. B **53**, 15932 (1996); S. A. Gurvitz, *ibid.* **57**, 6602 (1998).
[25] The occupation numbers of electrons, $n_L + n_R/2$ in particular, can be measured by using the charge sensing techniques, i.e., by using a quantum point contact near the DQD device to measure the conductance of the QPC. For details, see Refs. 16 and 17.
[26] H. Safar, P. L. Gammel, D. A. Huse, D. J. Bishop, J. P. Rice, and D. M. Ginsberg, Phys. Rev. Lett. **69**, 824 (1992).